Regular Article

blood

LYMPHOID NEOPLASIA

The amyloidogenic light chain is a stressor that sensitizes plasma cells to proteasome inhibitor toxicity

Laura Oliva,[1] Ugo Orfanelli,[1] Massimo Resnati,[1] Andrea Raimondi,[2] Andrea Orsi,[3] Enrico Milan,[1] Giovanni Palladini,[4,5] Paolo Milani,[4,5] Fulvia Cerruti,[6] Paolo Cascio,[6] Simona Casarini,[4,5] Paola Rognoni,[4,5] Thierry Touvier,[7] Magda Marcatti,[8] Fabio Ciceri,[8,9] Silvia Mangiacavalli,[10] Alessandro Corso,[10] Giampaolo Merlini,[4,5] and Simone Cenci[1,9]

[1]Unit of Age Related Diseases, Division of Genetics and Cell Biology, [2]Imaging Research Center, and [3]Unit of Protein Transport and Secretion, Division of Genetics and Cell Biology, San Raffaele Scientific Institute, Milan, Italy; [4]Amyloidosis Research and Treatment Center, Fondazione Istituto di Ricovero e Cura a Carattere Scientifico (IRCCS) Policlinico San Matteo, Pavia, Italy; [5]Department of Molecular Medicine, University of Pavia, Pavia, Italy; [6]Department of Veterinary Sciences, University of Turin, Turin, Italy; [7]Unit of Biology of Myelin, Division of Genetics and Cell Biology, and [8]Hematology and Bone Marrow Transplantation Unit, Department of Oncohematology, San Raffaele Scientific Institute, Milan, Italy; [9]Università Vita-Salute San Raffaele, Milan, Italy; and [10]Division of Hematology, Fondazione IRCCS Policlinico San Matteo, Pavia, Italy

Key Points

- Amyloidogenic PCs show unique PI susceptibility and altered organelle homeostasis, consistent with defective autophagy.
- Amyloidogenic LC production is an intrinsic cellular stressor that sensitizes to PI toxicity.

Systemic light chain (AL) amyloidosis is caused by the clonal production of an unstable immunoglobulin light chain (LC), which affects organ function systemically. Although pathogenic LCs have been characterized biochemically, little is known about the biology of amyloidogenic plasma cells (PCs). Intrigued by the unique response rates of AL amyloidosis patients to the first-in-class proteasome inhibitor (PI) bortezomib, we purified and investigated patient-derived AL PCs, in comparison with primary multiple myeloma (MM) PCs, the prototypical PI-responsive cells. Functional, biochemical, and morphological characterization revealed an unprecedented intrinsic sensitivity of AL PCs to PIs, even higher than that of MM PCs, associated with distinctive organellar features and expression patterns indicative of cellular stress. These consisted of expanded endoplasmic reticulum (ER), perinuclear mitochondria, and a higher abundance of stress-related transcripts, and were consistent with reduced autophagic control of organelle homeostasis. To test whether PI sensitivity stems from AL LC production, we engineered PC lines that can be induced to express amyloidogenic and nonamyloidogenic LCs, and found that AL LC expression alters cell growth and proteostasis and confers PI sensitivity. Our study discloses amyloidogenic LC production as an intrinsic PC stressor, and identifies stress-responsive pathways as novel potential therapeutic targets. Moreover, we contribute a cellular disease model to dissect the biology of AL PCs. (*Blood*. 2017; 129(15):2132-2142)

Introduction

Systemic light chain (AL) amyloidosis is a plasma cell (PC) dyscrasia caused by aggregation-prone monoclonal immunoglobulin light chains (LCs) produced by small clones of bone marrow (BM) PCs. These mutated, unstable LCs form insoluble β-pleated sheets that aggregate and deposit systemically in organ tissues as amyloid fibrils, causing organ dysfunction and death.[1-3] Heart involvement is the key determinant of survival, as patients with severe cardiac amyloidosis showed a median survival of only 4.4 months.[4] AL amyloidosis treatments are generally adapted from multiple myeloma (MM), the prototypical PC cancer.[5] Indeed, current regimens include immunomodulatory drugs (eg, thalidomide and lenalidomide) in combination with alkylating agents.[6-8] Proteasome inhibitors (PIs) have shown excellent clinical efficacy with unprecedented response rates, rapidly achieved in both previously untreated and pretreated patients.[9-11] However, a significant proportion of patients (40%) fail to respond.[12] The clinical efficacy of PIs raises the attractive possibility that the amyloidogenic PC clone, source of toxic LCs, is a direct target of PIs. If so, addressing the bases of PI sensitivity would define new targeted strategies to decrease drug toxicity and improve clinical outcome, containing and possibly eradicating the pathogenic clone.

We and others have demonstrated that large-scale immunoglobulin production is stressful to both normal and malignant PCs, and that defective protein homeostasis is a key determinant of the unique PI sensitivity of immunoglobulin-producing cells.[13-18] Here, we hypothesized that the biosynthesis of aggregation-prone LCs may further challenge protein homeostasis in the secretory pathway, inducing adaptive strategies in AL PCs whose identification could disclose more effective therapies against the amyloidogenic clone.

Although the small size of the AL amyloidosis PC clone in the BM hinders deep mechanistic biomolecular investigations,[1] to test our hypothesis we performed a functional and morphological characterization of a relatively large panel of primary, patient-derived PC

Submitted 14 August 2016; accepted 9 January 2017. Prepublished online as *Blood* First Edition paper, 27 January 2017; DOI 10.1182/blood-2016-08-730978.

G.M. and S. Cenci share senior authorship.

The online version of this article contains a data supplement.

There is an Inside *Blood* Commentary on this article in this issue.

The publication costs of this article were defrayed in part by page charge payment. Therefore, and solely to indicate this fact, this article is hereby marked "advertisement" in accordance with 18 USC section 1734.

samples. We compared AL PCs with primary MM PCs, the prototypical PI-responsive cells, and, in selected experiments, with PCs from individuals with monoclonal gammopathy of undetermined significance (MGUS), a MM-preceding clonal PC disorder genetically comparable to AL amyloidosis, but secreting nonamyloidogenic LCs.[19,20]

Our study revealed unique susceptibility of AL PCs to PIs, even higher than that of MM PCs, associated with distinctive organelle and expression features of stress. Moreover, to test the intrinsic effects of AL LC production on PC homeostasis, we engineered PC lines to express amyloidogenic and nonamyloidogenic LCs under control of an inducible promoter. Besides establishing cause-effect relationships, this system offers a valuable cellular model of AL amyloidosis for mechanistic and drug-screening studies.

Materials and methods

Patients

BM PCs were obtained from patients with AL amyloidosis (n = 43), MM (n = 25), or MGUS (n = 3) at diagnosis, prior to any chemotherapy (supplemental Table 1, available on the *Blood* Web site). The number of samples used in each set of experiments is indicated in Table 1.

Approval for use of primary samples was obtained from the Institutional Review Board of the San Raffaele Hospital and Fondazione IRCCS Policlinico San Matteo. Written consent was obtained from patients according to the Declaration of Helsinki.

Cell cultures

AL and MM PCs were enriched from BM aspirates through 2 rounds of CD138 immunomagnetic-positive selection (Easy Sep; StemCell Technologies, Vancouver, BC, Canada) and the percentage of $CD138^+$ cells verified by flow cytometry (AL, 78% ± 18%; MM, 85% ± 13%; P = not significant [NS]). Primary cells were cultured in RPMI 1640 medium (Gibco/Life Technologies) supplemented with 10% fetal calf serum, glutamax (1 mM), penicillin (100 U/mL), and streptomycin (100 μg/mL), in the absence of interleukin 6. Cell counts were performed with a Countess Automated Cell Counter (Invitrogen/Life Technologies).

Flow cytometric analyses of apoptosis

Patient-derived AL and MM PCs were seeded at 3×10^4 cells per 100 μL of medium in 96 multiwell plates, and treated for 24 hours with the indicated doses of bortezomib (Btz) and leupeptin, harvested, stained with fluorescein isothiocyanate–conjugated annexin V and propidium iodide as per manufacturer's instructions (BD Biosciences, Franklin Lakes, NJ), and with allophycocyanin-conjugated CD138, and analyzed by Accuri C6 (BD Biosciences, San Jose, CA) for disappearance of $CD138^+$ cells and subsequent apoptosis. Fifty percent effective concentration (EC_{50}) values were determined by nonlinear regression (Prism 5.0; GraphPad Software). Spontaneous viability of AL and MM PCs was comparable (AL, 89% ± 7.5%; MM, 76% ± 19%; P = NS). Drug-induced toxicity was quantified by subtracting death in parallel untreated samples. In selected experiments, cell death was assayed by trypan blue exclusion.

Immunofluorescence

Patient-derived PCs were seeded on poly-L-lysine–coated slides, fixed with 3.7% formaldehyde for 10 minutes, and permeabilized with phosphate-buffered saline 0.1% Triton X-100 10 minutes at room temperature. Cells were stained with monoclonal anti-Ub antibody (Fk2 [Enzo Biochem Inc, Farmingdale, NY], 1:200, 1 hour room temperature), rabbit anti-κ, or anti-λ antisera (Dako, Glostrup, Denmark; 1:200), rinsed in phosphate-buffered saline, and stained with Alexa Fluor 488 goat anti-mouse immunoglobulin G (IgG; 1:200) or Alexa Fluor 546 goat anti-rabbit IgG (1:500) and Hoechst 33342 (Molecular Probes, Eugene, OR). Coverslips were observed on a DeltaVision workstation (Applied Precision, Issaquah, WA) with an Olympus IX70 camera (Center Valley, PA). Numerical aperture was 1.35 (40× lens) and images of primary AL and MM PCs were deconvoluted with SoftWorx 3.5.0 (Applied Precision). Fluorescence intensity was quantified automatically with IN Cell Investigator software (GE Healthcare, Piscataway, NJ).

Table 1. Number of samples used in each set of experiments

	AL	MM	MGUS
PI and autophagy inhibitor toxicity	10	8	
Proteasome load	5	6	
Proteasome capacity	10	7	
Autophagy characterization by EM	5	5	
ER assessment by EM	7	5	3
G6Pase EM cytochemistry	3	3	
Mitochondrial EM characterization	9	6	3
Transcript expression	8	7	

Proteasome activity

Cells were centrifuged and pellets incubated in ice-cold extraction buffer (50 mM Tris-HCl pH 7.5, 1 mM dithiothreitol, 250 mM sucrose, 5 mM $MgCl_2$, 0.5 mM EDTA, 2 mM adenosine triphosphate, 0.025% digitonin) for 5 minutes and centrifuged at 20 000 *g* for 30 minutes at 4°C. Proteasome-specific chymotryptic activity was assayed by the release of 7-amino-4-methylcoumarin from a fluorogenic substrate, as described.[13,15-17] Briefly, 100 μM Suc-LLVY-AMC (BACHEM, Bubendorf, Switzerland) in 20 mM Tris-HCl pH 7.5, 1 mM adenosine triphosphate, 2 mM $MgCl_2$, 0.2% bovine serum albumin was added to protein extracts, and fluorescence monitored continuously at 37°C with a Carry Eclipse spectrofluorimeter (VARIAN, Palo Alto, CA). Background nonproteasomal degradation was controlled for by addition of the PI epoxomycin (1 μM; Sigma).

Electron microscopy and G6Pase cytochemistry

For conventional electron microscopy (EM) and glucose-6-phosphatase (G6Pase) EM cytochemistry, cells were pelleted and processed as described.[21] Briefly, ultrathin sections were contrasted with uranyl acetate and lead citrate, observed with a Leo 912AB electron microscope (Zeiss) operating at 80 kV. Digital micrographs were captured with a 2k × 2k Proscan slow-scan charge-coupled device camera system (Proscan HSC2) controlled by the integrated software (Soft Imaging Software). In conventional EM analyses, micrographs of randomly selected cells were digitalized and endoplasmic reticulum (ER) measured by stereography counting of the cisternae intersecting the main cellular axes; the percentage of perinuclear mitochondria was arbitrarily estimated as the proportion of mitochondria within the inner one-half distance between the perinuclear and plasma membrane; mitochondrial area and perimeter were analyzed with ImageJ software (http://rsbweb.nih.gov/ij/). The mitochondrial circularity index was calculated as: 4π (area)/(perimeter)^2. All measurements were performed in cells with unequivocal PC morphology. In G6Pase EM cytochemistry, automated assessment of $G6Pase^+$ area was achieved by ImageJ software.

Quantitative reverse transcription PCR

RNA was extracted from 0.3×10^6 to 1×10^6 cells with TRIzol (Life Technologies) and 0.5 μg to 1 μg were retrotranscribed with SuperScript Vilo (Life Technologies). Quantitative polymerase chain reactions (PCRs) were run in triplicates of 10-μL mixtures of SYBR Green I Master Mix (Roche), 0.5 μM primers and template complementary DNA corresponding to 2.5 ng to 5 ng of the original RNA on a Roche LightCycler 480 machine. Histone H3 messenger RNA (mRNA) served as quantification reference. Amplification of PC-specific transcripts certified PC purity (supplemental Figure 1). Data were analyzed with Advanced Relative Quantification software. Primers are listed in supplemental Table 2.

Immunoblot analyses

Cells were lysed and analyzed as detailed in supplemental Methods.

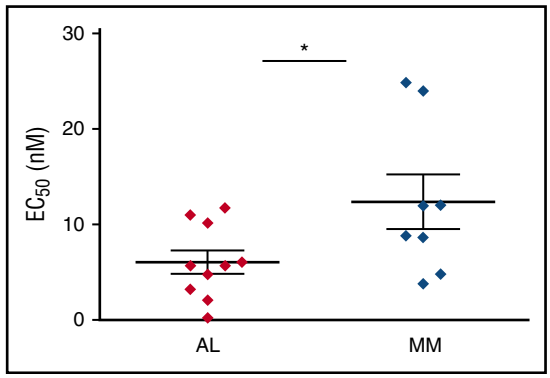

Figure 1. Primary AL amyloidosis PCs are significantly more susceptible to Btz toxicity than primary MM PCs. Primary PCs were purified by double immunomagnetic positive (CD138) selection from BM biopsies obtained from patients diagnosed with systemic light chain (AL) amyloidosis (n = 10) and MM (n = 8), seeded in multiwell plates and treated with increasing doses of Btz for 24 hours. Apoptotic responses were assessed by flow cytometric analysis, upon labeling with propidium iodide, fluorescent-conjugated anti-syndecan 1 antibody and annexin V. The graph shows each patient's average EC_{50}, and each group's mean ± standard error. *$P < .05$ (Student t test).

Generation and characterization of inducible LC-secreting cell lines

For doxycycline-inducible expression of AL and MM LCs, we used the lentiviral 1070-3T vector derived from the #1074 vector (kindly provided by L. Naldini, San Raffaele Scientific Institute, Milan, Italy).[22,23] Virus stocks were prepared as previously described.[24,25] The procedure is described in supplemental Methods. Construct maps are illustrated in supplemental Figure 2; LC sequences are available in supplemental Table 3.

Non-immunoglobulin-expressing NS0 murine plasmocytoma cells were transduced with lentiviral vector #1379 (kindly provided by L. Naldini),[26] cloned, and characterized as detailed in supplemental Methods.

Statistical and data analysis

Prism software (5.0; GraphPad) was used for data analysis. Statistical significance was tested with the 2-tailed Student t test ($P < .05$).

Results

Amyloidogenic PCs display intrinsic unique susceptibility to PIs

To investigate the intrinsic sensitivity of AL PCs to PIs, BM PCs were enriched from AL patients by double immunomagnetic positive selection for CD138 (syndecan-1), yielding on average 2×10^5 to 7×10^5 cells with substantial $CD138^+$ cell enrichment (78% ± 18%), as confirmed by selective amplification of PC-specific transcripts (supplemental Figure 1). Cells were then treated in vitro with increasing doses of the first-in-class PI Btz, and toxicity assayed. To unequivocally quantify cell death specifically within the PC population, we estimated the disappearance of $CD138^+$ cells, a marker whose loss is known to precede PC apoptosis with high sensitivity and specificity,[27,28] as we confirmed in primary PC samples (supplemental Figure 3). We found that patient-derived amyloidogenic PCs are not only intrinsically highly susceptible to Btz toxicity, but even significantly more sensitive than patient-purified MM cells, the prototypical PI-responsive cells (Figure 1). The intrinsic sensitivity of AL PCs raises the possibility that the mutated LC may act as a cell-autonomous stressor for PC proteostasis.

A load-vs-capacity imbalance does not account for the exquisite PI sensitivity of amyloidogenic PCs

The balance between proteasomal workload (ie, the overall amount of polyubiquitinated proteins requiring degradation) and total proteasomal capacity is a key determinant of PI responsiveness in normal and malignant PCs.[16-18] Therefore, we asked whether AL PCs display lower proteasome expression, higher proteasome workload, or both as compared with MM cells. To measure proteasomal capacity and workload, we respectively measured proteasome chymotryptic activity by specific fluorogenic substrate cleavage and accumulation of polyubiquitinated proteins by immunofluorescence, in primary AL and MM PCs, as described.[16,17] We found both workload and capacity comparable in primary AL and MM PCs (Figure 2). We excluded a significant contribution of BM cells other than PCs by measuring proteasome capacity of $CD138^-$ cells (supplemental Figure 4). Thus, the exquisite PI responsiveness of AL PCs is not accounted for by a more severe imbalance of proteasome function than that already reported in MM PCs.

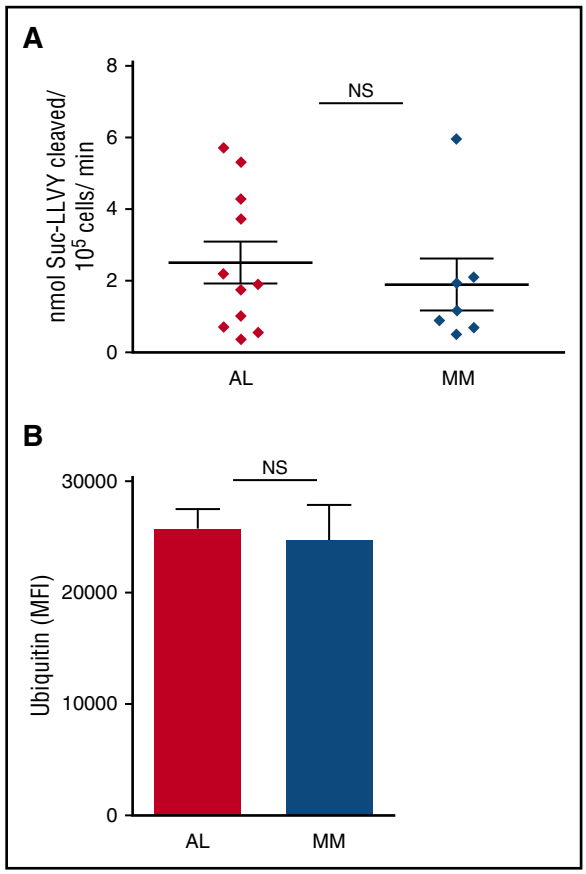

Figure 2. Comparable proteasome capacity and workload in primary PCs from AL amyloidosis and MM patients. Primary AL and MM PCs, purified as in Figure 1, were assayed in vitro for proteasome capacity (10 AL and 7 MM samples) and workload (5 AL and 6 MM samples). (A) Total cellular proteasome activity (capacity) was determined by means of an established fluorogenic peptide specifically probing the chymotryptic activity of the 20S proteolytic core (LLVY-amc), and expressed as peptide cleavage per total proteins over time. (B) Proteasome workload was estimated by automated, unbiased quantification of the intracellular accumulation of ubiquitinated proteins, upon immunofluorescent staining. Both graphs show each patient's average value, and each group's mean ± standard error (Student t test). MFI, mean fluorescence intensity.

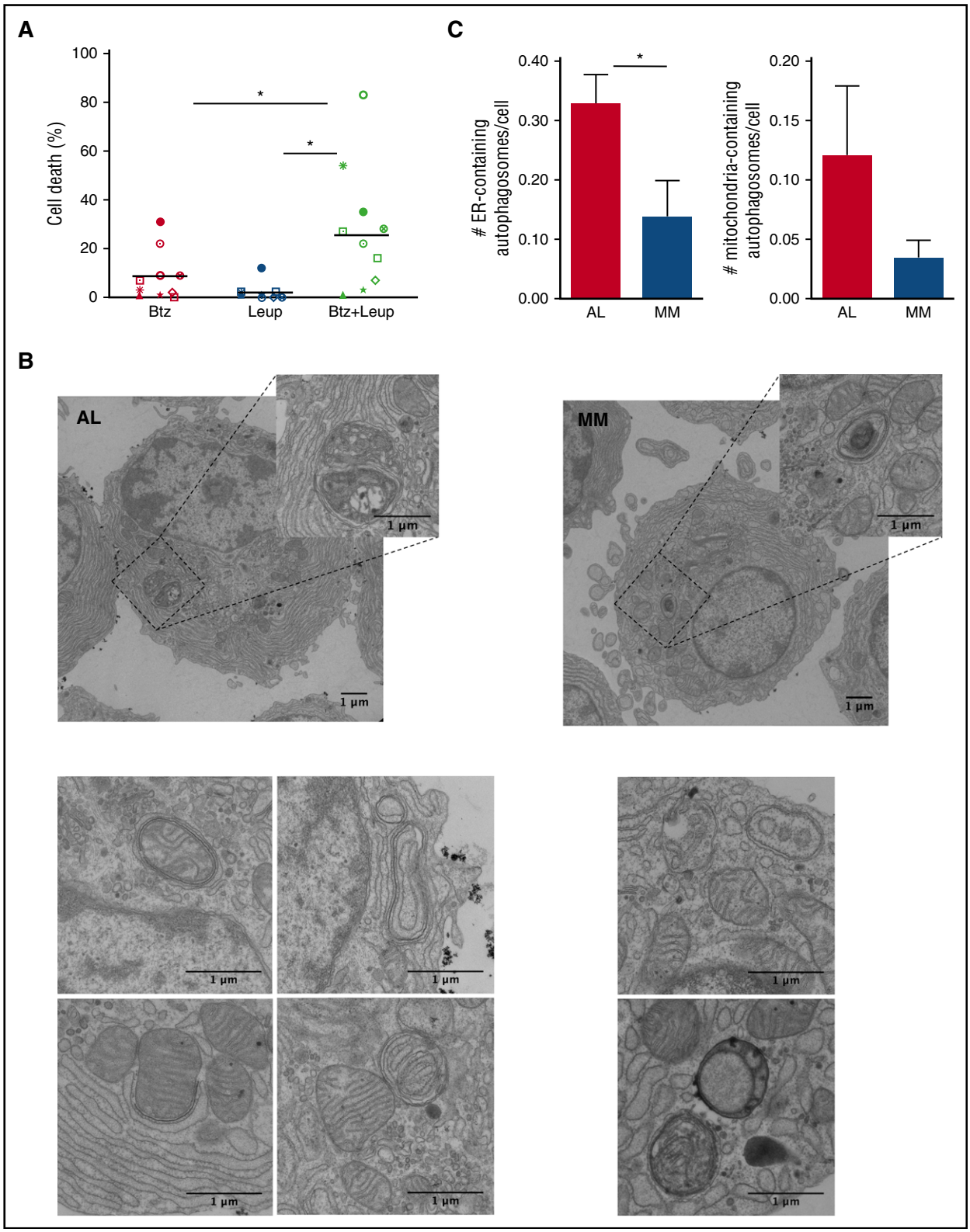

Figure 3. Abundant cytoprotective, organelle-homeostatic autophagy in primary amyloidogenic PCs. Assessment of autophagy and its role in primary AL PCs. (A) Proportion of cell death upon 24 hours of treatment with the distal autophagic inhibitor, leupeptin (Leup; 10 μM) and Btz (2 nM), alone or in combination, as assessed by cytofluorimetric analysis upon labeling with propidium iodide and fluorescent-conjugated antibody anti-syndecan 1 and annexin V. Each dot represents 1 of 10 AL patients. (B) EM analysis of autophagosomes in primary AL (left) and MM (right) PCs (representative images). (C) EM quantification of ER-phagy (left) and mitophagy (right) in AL and MM PCs. The histograms show the average numbers ± standard error of ER- and mitochondria-containing autophagosomes per PC in each AL and MM patient (>20 PCs per AL and MM patient; 5 patients per group). *$P < .05$ (Student t test).

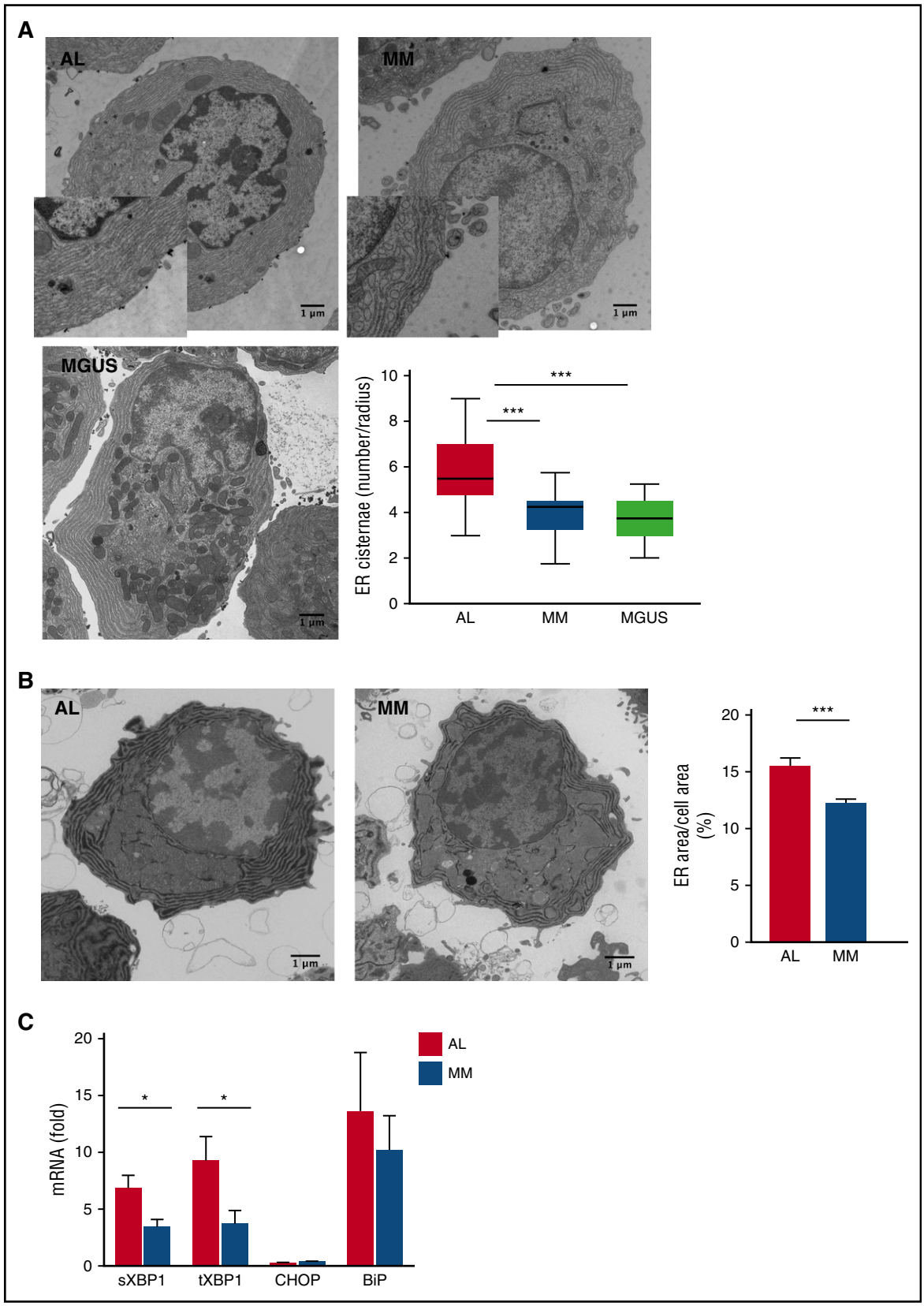

Figure 4. Perturbed ER homeostasis in primary amyloidogenic PCs. Assessment of ER abundance and homeostasis in primary PCs by EM (5-35 PCs per patient; 7 AL, 5 MM, and 3 MGUS patients per group) and G6Pase EM cytochemistry (>20 PCs per patient; 3 AL, 3 MM patients per group). (A) Representative EM images of BM PCs in AL, MM, and MGUS patients (insets: magnification ×1840), and quantification of ER size by stereography counting the number of ER cisternae intersecting the main cellular axes. Box plots show median, maximum, and minimum, and first and third quartile values. (B) Representative G6Pase EM cytochemistry images of BM PCs in AL and MM patients, and automated quantification of $G6Pase^{+}$ area (ER size), relative to total cell area (mean ± standard error). (C) Quantitative reverse transcription PCR analysis of transcripts encoding ER-stress responsive proteins (8 AL and 7 MM primary samples). Histograms show mean values ± standard error. ***$P < .0001$; *$P < .05$ (Student t test). BiP, immunoglobulin heavy chain binding protein; CHOP, CCAAT/enhancer-binding protein homologous protein; sXBP1, spliced X-box binding protein 1; tXBP1, total X-box binding protein 1.

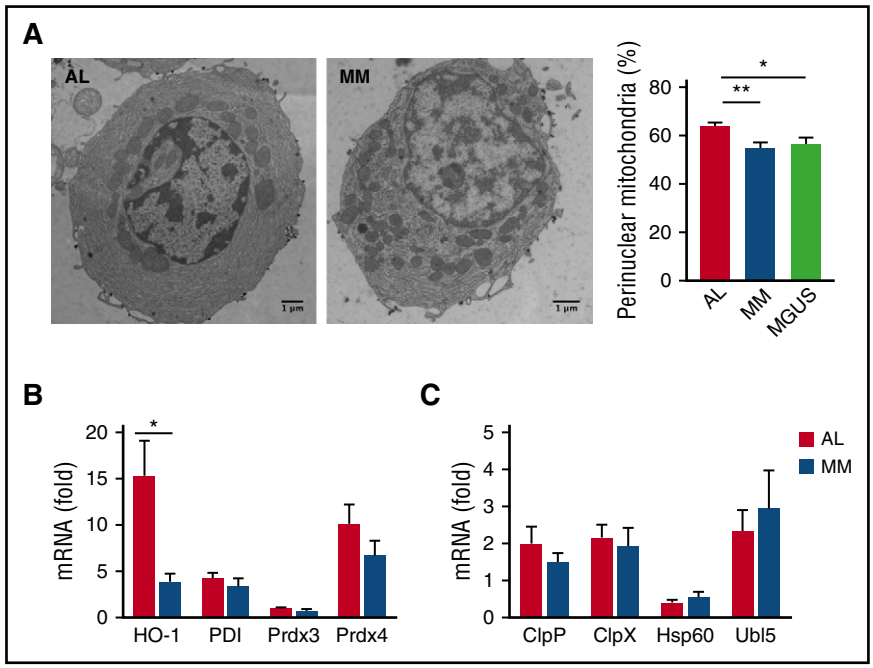

Figure 5. Mitochondrial stress in primary amyloidogenic PCs. Assessment of mitochondrial morphology and homeostasis in primary BM PCs purified from AL and MM patients by EM and transcripts analysis. (A) Representative EM images of BM PCs in AL, MM, and MGUS patients and analysis of cellular distribution of mitochondria. The percentage of perinuclear mitochondria was arbitrarily estimated as the proportion of mitochondria within half of the distance between perinuclear and plasma membrane (>20 PCs per patient; 9 AL, 6 MM, 3 MGUS primary samples per group). (B-C) Abundance of transcripts encoding HO-1 and organelle-resident redox sensors (B) and effectors of the mitochondrial UPR (C) assessed by quantitative reverse transcription PCR (8 AL and 7 MM patients). Histograms show mean values ± standard error. $^*P < .05$; $^{**}P < .005$ (Student *t* test). ClpP, caseinolytic mitochondrial matrix peptidase proteolytic subunit; ClpX, caseinolytic mitochondrial matrix peptidase chaperone subunit; Hsp60, heat shock protein 60; PDI, protein disulfide isomerase; Prdx3, peroxiredoxin 3; Prdx4, peroxiredoxin 4; Ubl5, ubiquitin-like 5.

Amyloidogenic PCs display intense autophagic activity, whose inhibition increases PI susceptibility

To investigate the cellular bases of the observed unique PI responsiveness of AL cells, we then examined other cellular pathways that cooperate with the ubiquitin-proteasome system (UPS) to maintain proteostasis. Macroautophagy, conventionally referred to as autophagy, is a selective lysosomal-recycling strategy known to collaborate with the UPS and to maintain organelle turnover and homeostasis.[29] We have recently demonstrated that autophagy is crucial in normal PCs to afford sustainable immunoglobulin production by controlling ER expansion.[21] Furthermore, we found that autophagy is a cell-autonomous absolute requirement to maintain the pool of resident BM PCs, the physiological counterpart of PC dyscrasias,[21] and that MM cells depend on autophagy for viability.[30] Finally, we and others have proposed that autophagy contributes to determine primary PI resistance of MM cells, as shown by the synergic toxicity of proteasome inhibition combined with genetic or pharmacological blockade of autophagy.[30-32] This background led us to hypothesize a role for autophagy in AL PC proteostasis and PI responsiveness.

To assess whether autophagy contributes to determine PI sensitivity of AL PCs, we treated primary AL PCs with a sublethal dose of Btz and with the distal autophagy inhibitor, leupeptin, alone or in combination, and found these treatments to exert significant synergic toxicity (Figure 3A). To further characterize autophagic activity in amyloidogenic PCs, we adopted EM, which enables the unbiased characterization of autophagosome abundance and content.[33] Extensive analyses of EM images of primary AL and MM PCs revealed a sizeable number of autophagosomes engulfing ER membranes and mitochondria, denoting active reticulophagy (ER-phagy) and mitophagy in both populations (Figure 3B). Notably, we found more ER- and mitochondria-containing autophagosomes in AL PCs than in MM cells (Figure 3C). Our data provide the first direct imaging of ER-phagy and mitophagy in AL PCs, and are in keeping with the organelle-homeostatic function of autophagy we recently demonstrated in normal and malignant PCs.[21,30]

Perturbed ER homeostasis in amyloidogenic PCs

We have previously reported that selective autophagy controls ER size and secretory homeostasis in normal PCs and MM cells.[21,30] The higher frequency of ER-containing autophagosomes observed in AL PCs may stem either from increased ER-phagy or from defective lysosomal digestion of ER-engulfing autophagosomes, which may impact on ER homeostasis. To test this hypothesis, we characterized the ER compartment using 2 independent approaches: EM and G6Pase EM cytochemistry.[21] These experiments unveiled significantly more abundant ER in AL PCs as compared with MM (Figure 4A-B). Attesting to a distinctive feature of amyloidogenic PCs, we found their ER to be also significantly more abundant than in PCs from individuals with MGUS (Figure 4A), a premalignant monoclonal gammopathy also caused by a small clone of low-proliferating PCs, which shares several chromosomal aberrations with AL.[20] Together with the higher frequency of ER-engulfing autophagosomes reported in the previous paragraph (Figure 3C), the data support the hypothesis of defective ER-phagy. The functional relevance of such alteration in AL PCs is demonstrated by significantly higher expression of spliced and total *XBP1* transcripts (Figure 4C), indicative of increased ER stress.[34] Notably, the activation of the protein kinase R–like ER kinase (PERK) branch of the unfolded protein response (UPR) was negligible, as witnessed by the low expression of its downstream mediator CHOP, in line with previous reports on PCs.[35,36] Taken together, the data demonstrate that ER homeostasis is perturbed in AL PCs, likely as a result of defective ER-phagy.

Amyloidogenic PCs display altered mitochondrial distribution

Having observed more abundant mitochondria-containing autophagosomes in AL than MM PCs (Figure 3B-C), we next checked whether mitochondrial homeostasis is also differentially affected in AL and MM primary PCs. EM analyses revealed a peculiar distribution of these organelles in AL PCs. Indeed, although mitochondrial area, average size, and circularity, an index of mitochondrial network fragmentation,[37] were comparable in AL and MM PCs (supplemental Figure 5), amyloidogenic PCs showed a significantly higher proportion of perinuclear mitochondria than MM and MGUS PCs (Figure 5A). Perinuclear distribution of mitochondria has been previously associated with oxidative stress.[38] Indeed, we found higher abundance of the heme oxygenase-1 (HO-1) transcript, a key effector of cellular antioxidant

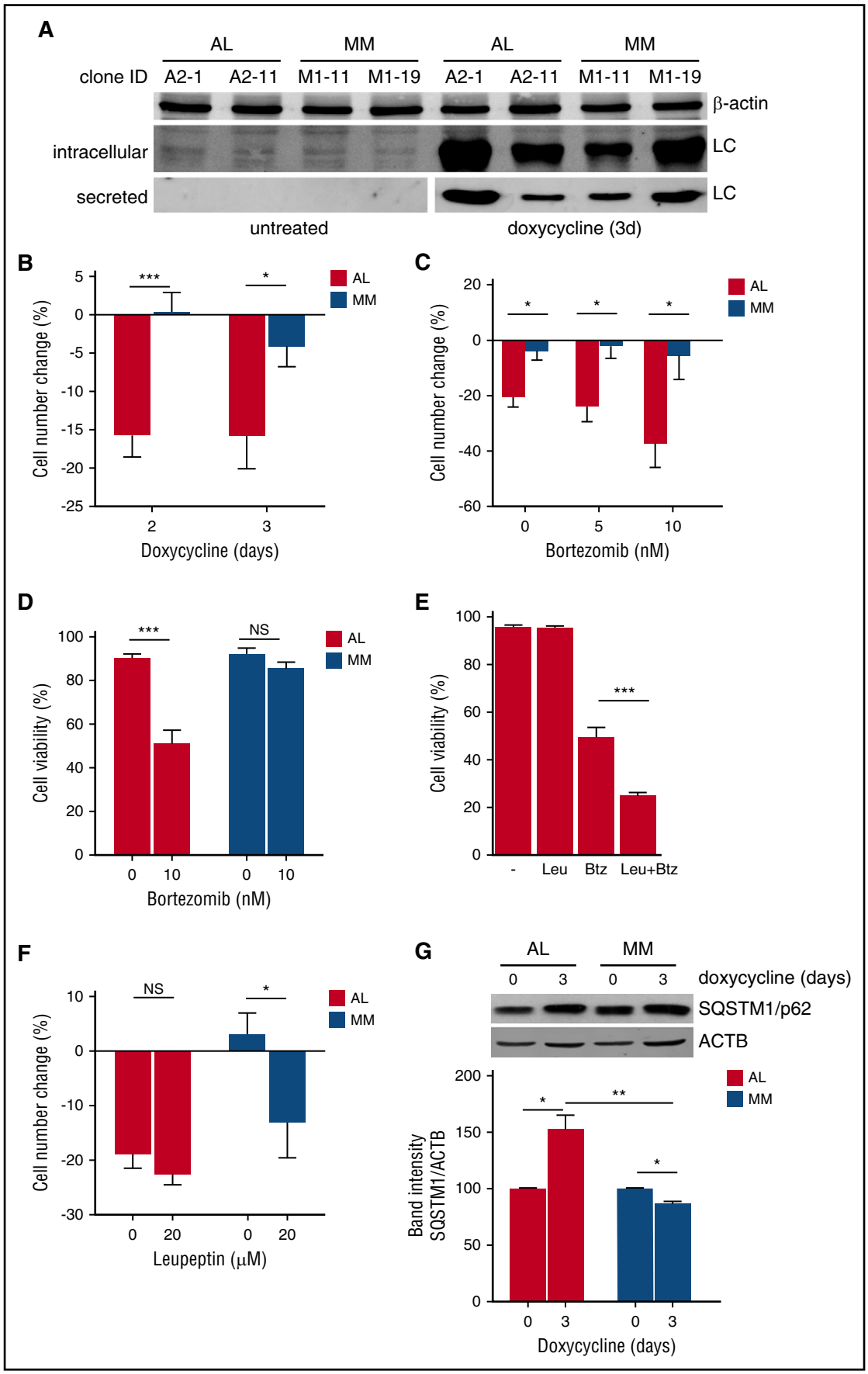

Figure 6.

responses,[39] in AL PCs (Figure 5B). Together, these findings are suggestive of distinctive oxidative stress associated with amyloidogenic LC production. However, expression of representative effectors of the mitochondrial UPR (UPR^{mt}), an adaptive response known to cope with mitochondrial dysfunction originating from different types of stress,[40,41] is not significantly different in AL and MM PCs (Figure 5C), attesting to overall maintained mitochondria homeostasis, and in line with the survival of amyloidogenic PC clones.

Amyloidogenic LC expression is an intrinsic stressor that sensitizes to PI toxicity

Having identified peculiar PI susceptibility and perturbed homeostasis of key organelle substrates of autophagy in AL PCs, we then adopted a reductionist approach to assess whether amyloidogenic LC production is sufficient to induce stress and PI susceptibility in a PC-autonomous fashion. Through lentiviral engineering, we generated PC clones expressing highly cardiotoxic amyloidogenic or nonamyloidogenic LCs, respectively cloned from 2 AL amyloidosis and 2 MM patients, under control of a doxycycline-inducible promoter. Inducible amyloidogenic (AL) and nonamyloidogenic (MM) PC lines were generated from NS0 cells, a non-LC-synthesizing, non-immunoglobulin-secreting murine plasmocytoma, and different clones selected for efficient AL and MM LC mRNA and protein expression and secretion. All clones survived in vitro when induced to produce LC (not shown), in keeping with the clinical notion that PC clones producing toxic AL LCs are maintained in patients' BM. Figure 6A shows immunoblot analyses on 1 AL and 1 MM cell line, demonstrating effective induction of intracellular expression and secretion of both LCs by representative clones of both lines. We then compared cell growth and PI sensitivity in clones that displayed comparable LC expression, as quantified by enzyme-linked immunosorbent assay and nephelometry. Although all clones showed superimposable growth curves in absence of doxycycline, upon induction of LC expression, amyloidogenic clones showed lower cell growth rates as compared with nonamyloidogenic counterparts (Figure 6B; supplemental Figure 6A), with no difference in cell viability (not shown). Furthermore, treatment with Btz not only aggravated the cell growth defect, but also reduced cell viability selectively in AL LC-expressing PCs (Figure 6C-D; supplemental Figure 6B). Engineered amyloidogenic cell lines revealed synergic toxicity of combined proteasome and autophagy inhibition (Figure 6E), confirming the key proteostatic role of autophagy already observed in primary amyloidogenic PCs (Figure 3A). Moreover, attesting to a causal role for insufficient autophagy, the cell growth defect observed in PCs engineered to express the AL LC was recapitulated in nonamyloidogenic PCs by autophagic inhibition (Figure 6F). In line with this hypothesis, AL, but not MM LC, expression induced significant accumulation of the autophagic substrate SQSTM1/p62, indicative of insufficient autophagy (Figure 6G).[30,42] Altogether, the data provide formal evidence that expression of an amyloidogenic LC is an intrinsic stressor sufficient to perturb cellular proteostasis and to sensitize to PI toxicity, at least partially by saturating the cellular autophagic reserve.

Discussion

Clinical studies have demonstrated that AL amyloidosis patients are particularly responsive to PI treatment,[9] even more than patients with MM, the prototypical PI-responsive cancer, suggesting an exquisite intrinsic sensitivity of AL PCs to negative proteostasis modulators.[9-12,43,44] Identifying intrinsic weaknesses of AL PCs and understanding the underlying bases hold promise for defining new strategies to enhance therapeutic efficacy, but direct studies of amyloidogenic PCs have been hindered so far by the relative rarity of the cell population. Here, we set out to characterize, for the first time, primary AL PCs functionally, biochemically, and morphologically, investigating cellular proteostasis, PI sensitivity, organelle morphology, and stress responses. The data collected reveal an intrinsic high vulnerability of AL PCs to PIs, even higher than that of MM PCs (Figure 1), so far considered the prototypic PI-susceptible cells.

In previous works, we have proposed the balance between proteasome workload and capacity as a critical determinant of PI sensitivity in both normal and malignant PCs.[13,16,17] In particular, in MM lines and myeloma patient-derived PCs, PI vulnerability was found to correlate directly with the load of ubiquitinated proteins requiring degradation, and inversely with overall proteasome activity; moreover, increasing proteasome biogenesis or workload significantly affected PI sensitivity.[16,17] This evidence led to the currently established load-vs-capacity model of PI sensitivity.[18] We first asked whether such a model may explain the exquisite vulnerability of AL PCs. However, the assessment of ubiquitin-conjugated proteins by immunofluorescence and of total proteasome activity by specific fluorogenic substrate cleavage revealed comparable proteasome load and capacity in primary PCs purified from AL and MM patients (Figure 2). These findings prompted us to search for alternative biological bases underlying the exquisite PI sensitivity of AL PCs.

We hypothesized that the amyloidogenic LC poses a more severe burden than the normal LC on PC proteostasis by interfering with autophagy, a lysosomal proteocatabolic strategy capable of alleviating proteasome workload.[45-48] Indeed, we recently demonstrated that autophagy is absolutely required in mice to maintain BM long-lived PCs, normal counterparts of PC dyscrasias.[21] Of note, we also reported that autophagy controls organelle homeostasis and sustains PI resistance and cell survival in MM cells.[30] In keeping with a key homeostatic function of autophagy in AL PCs, our EM analyses

Figure 6. Amyloidogenic LC expression is an intrinsic cellular stressor. Effect of expression of amyloidogenic (AL) and nonamyloidogenic (MM) LC on PC growth, PI sensitivity, and autophagy. (A) The non-immunoglobulin-expressing NS0 murine plasmocytoma cell line was lentivirally engineered to express amyloidogenic and nonamyloidogenic immunoglobulin LCs under control of an inducible promoter, and clones selected and characterized for LC expression. Effective induction of LC expression and secretion by doxycycline (1 μM for 3 days) in 2 representative clones is shown in 1 representative immunoblot analysis. (B) AL and MM NS0 clones were treated with 1 μM doxycycline or left untreated for the indicated days. The number of viable cells upon induction of LC production by doxycycline and in untreated cultures was determined every 24 hours by trypan blue exclusion. The effect of LC induction on cell growth as compared with parallel, untreated cultures was expressed as percentage of cell number change. The histogram shows the average of 2 AL (A2-1 and A2-11) and 2 MM (M1-11 and M1-19) NS0 clones. (C) AL (A2-1) and MM (M1-19) NS0 clones were induced to express the respective LC for 3 days and the effect on cell growth of the indicated doses of Btz administered for the last day evaluated as in panel B. (D) Analysis of cell viability 3 days post-LC induction in the experiment in panel C. (E) A2-1 cells were induced to express the amyloidogenic LC for 3 days and the effect on cell viability of treatment with the distal autophagic inhibitor, leupeptin (Leu, 20 μM for the last 48 hours) and Btz (10 nM for the last 24 hours), alone or in combination, assayed by trypan blue exclusion (average of 4 independent experiments). (F) AL (A2-1) and MM (M1-19) NS0 clones were induced to express the respective LC for 3 days and the effect on cell growth of the indicated dose of leupeptin for the last 48 hours evaluated as in panel B. (G) The effect of 3 days induction of AL and MM LC on the accumulation of autophagic substrate SQSTM1/p62 assessed by immunoblotting. Top panel: one representative image; histogram: quantification of 3 independent experiments. Results are expressed as mean ± standard error of the mean (SEM) of at least 3 independent experiments. $^{*}P < .05$; $^{***}P < .001$ (2-tailed Student *t* test).

revealed numerous autophagosomes engulfing ER and mitochondria (Figure 3). Moreover, morphological and functional assessment revealed substantial differences between primary AL and MM cells, with perturbed ER and mitochondrial homeostasis and coherent transcriptional signatures of stress in amyloidogenic PCs (Figures 4 and 5). These findings are consistent with defective autophagy in primary AL PCs.

To investigate whether the organellar stress features identified are distinctive of amyloidogenic PCs, in EM studies of cellular morphology we also included primary PCs from patients with MGUS, also caused by a small clone of low-proliferating PCs, sharing several chromosomal aberrations with AL.[20] Indeed, more abundant ER and perinuclear mitochondria were found to be associated with amyloidogenic LC production (Figures 4 and 5), encouraging us to further explore the intrinsic effects of AL LC expression in PCs.

In vivo and in vitro studies have shown that once secreted, the amyloidogenic LC can cause end-organ damage by interfering with autophagy in target cells. In particular, AL LC may cause accumulation of dysfunctional mitochondria and toxic reactive oxygen species, possibly by impairing autophagic clearance in cardiomyocytes.[49] Our data support the novel possibility that the amyloidogenic LC may burden protein homeostasis even before being secreted, thereby harming the PC itself. The observed higher UPR, the adaptive pathway counteracting altered ER proteostasis,[34] together with signs of oxidative stress, namely higher expression of the canonical antioxidant response factor, HO-1,[39] and perinuclear mitochondria distribution,[38] further attest to a stressful intracellular environment in AL PCs. Our data integrate with previous functional gene expression analyses that disclosed a molecular signature including transcripts implicated in protein processing and folding differentially expressed in AL PCs as compared with MM PCs.[50]

The mechanism whereby the amyloidogenic LC may stress cellular homeostasis is challenging. An intriguing possibility is that the aggregation-prone LC may generate intracellular toxic aggregate species that interact aberrantly with various factors of the proteostasis network, including chaperones, components of the UPS and autophagy, eventually resulting in cellular stress and proteostasis impairment.[51,52] Notably, we have previously excluded a role for autophagy in the clearance of immunoglobulin molecules in normal and malignant PCs.[21,30,53] Our data suggest that, unlike normal LCs, aggregation-prone LCs may be selectively targeted by autophagy, at the expense of constitutive organelle homeostasis, ultimately leading to cellular stress. A recent clinical study disclosed poorer outcome of AL patients with translocation t(11;14) treated with bortezomib-based regimens.[54] Our findings on primary AL PCs encourage investigation of the protein and organelle homeostatic features of PCs from patients carrying t(11;14).

To conclusively test whether production of an amyloidogenic LC is sufficient to induce cellular stress, we engineered the non-immunoglobulin-expressing murine plasmocytoma NS0 to stably express highly cardiotoxic amyloidogenic and normal LCs, respectively cloned from AL and MM patients. To minimize cellular adaptation and better gauge the effects of LC production, we exploited an efficient doxycycline-inducible promoter. Doxycycline has been shown to possess antiaggregation activity; however, such activity is achieved at doses >25 times higher than the maximum concentration (1 μM) used herein to induce LC transgene expression.[55,56] Moreover, we excluded our treatment to affect accumulation of polyubiquitinated proteins in LC-expressing NS0 clones (data not shown). Our model revealed a significant impact of amyloidogenic LC production on PC homeostasis. Such an effect was subtle, consistent with the clinical evidence that the amyloidogenic clone is maintained in the BM, and with the chronic nature of the disease. However, we found that AL LC production limited cellular growth (Figure 6; supplemental Figure 6). Attesting to a causal role of autophagy, a similar growth defect was obtained by autophagy inhibition in nonamyloidogenic LC-producing PCs; selective accumulation of the autophagy substrate SQSTM1/p62 upon AL LC induction further supported a role for impaired autophagy in AL clones (Figure 6). The observed reduction in cell growth was not associated with enhanced cell death, suggesting that decreased proliferation may represent an adaptive strategy sustaining the maintenance of the stressed clone. On the other hand, production of the amyloidogenic LC sensitized PCs to PI toxicity, recapitulating the phenotype observed in primary AL PCs (Figure 6; supplemental Figure 6).

Although inevitably artificial, the reductionist mouse cell line model presented herein engineered to express human patient-derived LCs fulfills the need of a cellular model of AL amyloidosis, as only 1 patient-derived AL cell line is currently available for research.[57] Among other advantages, by expressing AL and non-AL LCs in the same genetic and cellular background, our model enables direct ascription of biological differences to the expression of a specific LC.

In summary, we characterized, for the first time, primary patient-derived AL PCs biochemically, morphologically, and functionally, and identified unique stress features, suggestive of impaired autophagic maintenance of organelle homeostasis. These insights in the unique biology of amyloidogenic PCs may offer new therapeutic targets against the toxic pathogenic clone. Moreover, we have engineered the first cellular model of inducible amyloidogenic PCs as a preclinical tool to characterize the intracellular effects of amyloidogenic LC production and identify more effective therapeutic agents against AL amyloidosis.

Acknowledgments

The authors thank Federica Loro for assistance and the Cenci laboratory members for creative discussions. The authors are particularly grateful to: Riccardo Albertini, Anush Bakunts, Tiziana Bosoni, Stefano Casola, Monica Fabbri, Moshe Gatt, Luigi Naldini, Gabriella Passerini, Niccolò Pengo, Laura Pirolini, Fulvio Reggiori, Alessandra Romano, Roberto Sitia, Veronica Valentini, and Eelco van Anken.

This work was supported by a 2014 Brian D. Novis Research Award by the International Myeloma Foundation (L.O.) and by grants from the Multiple Myeloma Research Foundation (Senior Research Award 2010), the Italian Ministry of Health (Giovani Ricercatori 1143560), and the Associazione Italiana per la Ricerca sul Cancro (AIRC; Investigator Grants 14691 and 18858, and Special Program Molecular Clinical Oncology 5 per mille n. 9965) (S.Cenci). G.M. was supported by AIRC (Special Program Molecular Clinical Oncology 5 per mille n. 9965), Fondazione Cariplo (2013-0964), and the Italian Ministry of Health (GR-2010-2317596 and RF-2013-02355259).

Authorship

Contribution: S. Cenci, G.M., and L.O. designed experiments; L.O., U.O., M.R., A.R., A.O., E.M., F. Cerruti, P.C., P.R., and T.T. did the experiments; G.P., P.M., S. Casarini, M.M., F. Ciceri, S.M., A.C.,

and G.M. provided and characterized patient samples; and L.O., S.Cenci, and G.M. analyzed data and wrote the paper.

Conflict-of-interest disclosure: G.M. received honoraria from Takeda and Janssen-Cilag. The remaining authors declare no competing financial interests.

ORCID profiles: S.Cenci, 0000-0003-1215-7518.

Correspondence: Simone Cenci, DiBiT 4A1, Room 18A, San Raffaele Scientific Institute, Via Olgettina 58, 20132 Milan, Italy; e-mail: cenci.simone@hsr.it; and Giampaolo Merlini, Centro per lo Studio e la Cura delle Amiloidosi Sistemiche, Fondazione IRCCS Policlinico San Matteo and University of Pavia, Viale Golgi 19, 27100 Pavia, Italy; e-mail: gmerlini@unipv.it.

References

1. Merlini G, Stone MJ. Dangerous small B-cell clones. *Blood*. 2006;108(8):2520-2530.
2. Lebovic D, Hoffman J, Levine BM, et al. Predictors of survival in patients with systemic light-chain amyloidosis and cardiac involvement initially ineligible for stem cell transplantation and treated with oral melphalan and dexamethasone. *Br J Haematol*. 2008;143(3):369-373.
3. Dietrich S, Schönland SO, Benner A, et al. Treatment with intravenous melphalan and dexamethasone is not able to overcome the poor prognosis of patients with newly diagnosed systemic light chain amyloidosis and severe cardiac involvement. *Blood*. 2010;116(4):522-528.
4. Merlini G, Palladini G. Treating advanced cardiac damage in light chain amyloidosis: still an unmet need. *Haematologica*. 2014;99(9):1407-1409.
5. Merlini G, Seldin DC, Gertz MA. Amyloidosis: pathogenesis and new therapeutic options. *J Clin Oncol*. 2011;29(14):1924-1933.
6. Wechalekar AD, Goodman HJ, Lachmann HJ, Offer M, Hawkins PN, Gillmore JD. Safety and efficacy of risk-adapted cyclophosphamide, thalidomide, and dexamethasone in systemic AL amyloidosis. *Blood*. 2007;109(2):457-464.
7. Kastritis E, Terpos E, Roussou M, et al. A phase 1/2 study of lenalidomide with low-dose oral cyclophosphamide and low-dose dexamethasone (RdC) in AL amyloidosis. *Blood*. 2012;119(23):5384-5390.
8. Kumar SK, Hayman SR, Buadi FK, et al. Lenalidomide, cyclophosphamide, and dexamethasone (CRd) for light-chain amyloidosis: long-term results from a phase 2 trial. *Blood*. 2012;119(21):4860-4867.
9. Kastritis E, Wechalekar AD, Dimopoulos MA, et al. Bortezomib with or without dexamethasone in primary systemic (light chain) amyloidosis. *J Clin Oncol*. 2010;28(6):1031-1037.
10. Venner CP, Gillmore JD, Sachchithanantham S, et al. A matched comparison of cyclophosphamide, bortezomib and dexamethasone (CVD) versus risk-adapted cyclophosphamide, thalidomide and dexamethasone (CTD) in AL amyloidosis. *Leukemia*. 2014;28(12):2304-2310.
11. Palladini G, Milani P, Foli A, et al. Melphalan and dexamethasone with or without bortezomib in newly diagnosed AL amyloidosis: a matched case-control study on 174 patients. *Leukemia*. 2014;28(12):2311-2316.
12. Palladini G, Sachchithanantham S, Milani P, et al. A European collaborative study of cyclophosphamide, bortezomib, and dexamethasone in upfront treatment of systemic AL amyloidosis. *Blood*. 2015;126(5):612-615.
13. Cenci S, Mezghrani A, Cascio P, et al. Progressively impaired proteasomal capacity during terminal plasma cell differentiation. *EMBO J*. 2006;25(5):1104-1113.
14. Meister S, Schubert U, Neubert K, et al. Extensive immunoglobulin production sensitizes myeloma cells for proteasome inhibition. *Cancer Res*. 2007;67(4):1783-1792.
15. Cascio P, Oliva L, Cerruti F, et al. Dampening Ab responses using proteasome inhibitors following in vivo B cell activation. *Eur J Immunol*. 2008;38(3):658-667.
16. Bianchi G, Oliva L, Cascio P, et al. The proteasome load versus capacity balance determines apoptotic sensitivity of multiple myeloma cells to proteasome inhibition. *Blood*. 2009;113(13):3040-3049.
17. Cenci S, Oliva L, Cerruti F, et al. Pivotal advance: protein synthesis modulates responsiveness of differentiating and malignant plasma cells to proteasome inhibitors. *J Leukoc Biol*. 2012;92(5):921-931.
18. Cenci S. The proteasome in terminal plasma cell differentiation. *Semin Hematol*. 2012;49(3):215-222.
19. Merlini G, Palladini G. Differential diagnosis of monoclonal gammopathy of undetermined significance. *Hematology Am Soc Hematol Educ Program*. 2012;2012:595-603.
20. Bochtler T, Hegenbart U, Cremer FW, et al. Evaluation of the cytogenetic aberration pattern in amyloid light chain amyloidosis as compared with monoclonal gammopathy of undetermined significance reveals common pathways of karyotypic instability. *Blood*. 2008;111(9):4700-4705.
21. Pengo N, Scolari M, Oliva L, et al. Plasma cells require autophagy for sustainable immunoglobulin production. *Nat Immunol*. 2013;14(3):298-305.
22. Gentner B, Visigalli I, Hiramatsu H, et al. Identification of hematopoietic stem cell-specific miRNAs enables gene therapy of globoid cell leukodystrophy. *Sci Transl Med*. 2010;2(58):58ra84.
23. Chiriaco M, Farinelli G, Capo V, et al. Dual-regulated lentiviral vector for gene therapy of X-linked chronic granulomatosis. *Mol Ther*. 2014;22(8):1472-1483.
24. Dull T, Zufferey R, Kelly M, et al. A third-generation lentivirus vector with a conditional packaging system. *J Virol*. 1998;72(11):8463-8471.
25. Follenzi A, Ailles LE, Bakovic S, Geuna M, Naldini L. Gene transfer by lentiviral vectors is limited by nuclear translocation and rescued by HIV-1 pol sequences. *Nat Genet*. 2000;25(2):217-222.
26. Amendola M, Venneri MA, Biffi A, Vigna E, Naldini L. Coordinate dual-gene transgenesis by lentiviral vectors carrying synthetic bidirectional promoters. *Nat Biotechnol*. 2005;23(1):108-116.
27. Jourdan M, Ferlin M, Legouffe E, et al. The myeloma cell antigen syndecan-1 is lost by apoptotic myeloma cells. *Br J Haematol*. 1998;100(4):637-646.
28. Nerini-Molteni S, Ferrarini M, Cozza S, Caligaris-Cappio F, Sitia R. Redox homeostasis modulates the sensitivity of myeloma cells to bortezomib. *Br J Haematol*. 2008;141(4):494-503.
29. Mizushima N, Komatsu M. Autophagy: renovation of cells and tissues. *Cell*. 2011;147(4):728-741.
30. Milan E, Perini T, Resnati M, et al. A plastic SQSTM1/p62-dependent autophagic reserve maintains proteostasis and determines proteasome inhibitor susceptibility in multiple myeloma cells. *Autophagy*. 2015;11(7):1161-1178.
31. Hoang B, Benavides A, Shi Y, Frost P, Lichtenstein A. Effect of autophagy on multiple myeloma cell viability. *Mol Cancer Ther*. 2009;8(7):1974-1984.
32. Santo L, Hideshima T, Kung AL, et al. Preclinical activity, pharmacodynamic, and pharmacokinetic properties of a selective HDAC6 inhibitor, ACY-1215, in combination with bortezomib in multiple myeloma. *Blood*. 2012;119(11):2579-2589.
33. Klionsky DJ, Abdalla FC, Abeliovich H, et al. Guidelines for the use and interpretation of assays for monitoring autophagy. *Autophagy*. 2012;8(4):445-544.
34. Walter P, Ron D. The unfolded protein response: from stress pathway to homeostatic regulation. *Science*. 2011;334(6059):1081-1086.
35. Skalet AH, Isler JA, King LB, Harding HP, Ron D, Monroe JG. Rapid B cell receptor-induced unfolded protein response in nonsecretory B cells correlates with pro- versus antiapoptotic cell fate. *J Biol Chem*. 2005;280(48):39762-39771.
36. Masciarelli S, Fra AM, Pengo N, et al. CHOP-independent apoptosis and pathway-selective induction of the UPR in developing plasma cells. *Mol Immunol*. 2010;47(6):1356-1365.
37. Raimondi A, Mangolini A, Rizzardini M, et al. Cell culture models to investigate the selective vulnerability of motoneuronal mitochondria to familial ALS-linked G93ASOD1. *Eur J Neurosci*. 2006;24(2):387-399.
38. Al-Mehdi AB, Pastukh VM, Swiger BM, et al. Perinuclear mitochondrial clustering creates an oxidant-rich nuclear domain required for hypoxia-induced transcription. *Sci Signal*. 2012;5(231):ra47.
39. Choi AM, Alam J. Heme oxygenase-1: function, regulation, and implication of a novel stress-inducible protein in oxidant-induced lung injury. *Am J Respir Cell Mol Biol*. 1996;15(1):9-19.
40. Zhao Q, Wang J, Levichkin IV, Stasinopoulos S, Ryan MT, Hoogenraad NJ. A mitochondrial specific stress response in mammalian cells. *EMBO J*. 2002;21(17):4411-4419.
41. Haynes CM, Fiorese CJ, Lin YF. Evaluating and responding to mitochondrial dysfunction: the mitochondrial unfolded-protein response and beyond. *Trends Cell Biol*. 2013;23(7):311-318.
42. Johansen T, Lamark T. Selective autophagy mediated by autophagic adapter proteins. *Autophagy*. 2011;7(3):279-296.
43. Reece DE, Hegenbart U, Sanchorawala V, et al. Long-term follow-up from a phase 1/2 study of single-agent bortezomib in relapsed systemic AL amyloidosis. *Blood*. 2014;124(16):2498-2506.
44. Landau H, Hassoun H, Rosenzweig MA, et al. Bortezomib and dexamethasone consolidation following risk-adapted melphalan and stem cell transplantation for patients with newly diagnosed light-chain amyloidosis. *Leukemia*. 2013;27(4):823-828.
45. Pandey UB, Nie Z, Batlevi Y, et al. HDAC6 rescues neurodegeneration and provides an essential link between autophagy and the UPS. *Nature*. 2007;447(7146):859-863.
46. Aronson LI, Davies FE. DangER: protein ovERload. Targeting protein degradation to treat myeloma. *Haematologica*. 2012;97(8):1119-1130.
47. He C, Klionsky DJ. Regulation mechanisms and signaling pathways of autophagy. *Annu Rev Genet*. 2009;43:67-93.
48. Kroemer G, Mariño G, Levine B. Autophagy and the integrated stress response. *Mol Cell*. 2010;40(2):280-293.

49. Guan J, Mishra S, Qiu Y, et al. Lysosomal dysfunction and impaired autophagy underlie the pathogenesis of amyloidogenic light chain-mediated cardiotoxicity. *EMBO Mol Med*. 2014; 6(11):1493-1507.

50. Abraham RS, Ballman KV, Dispenzieri A, et al. Functional gene expression analysis of clonal plasma cells identifies a unique molecular profile for light chain amyloidosis. *Blood*. 2005;105(2): 794-803.

51. Olzscha H, Schermann SM, Woerner AC, et al. Amyloid-like aggregates sequester numerous metastable proteins with essential cellular functions. *Cell*. 2011;144(1):67-78.

52. Hipp MS, Park SH, Hartl FU. Proteostasis impairment in protein-misfolding and -aggregation diseases. *Trends Cell Biol*. 2014;24(9):506-514.

53. Auner HW, Cenci S. Recent advances and future directions in targeting the secretory apparatus in multiple myeloma. *Br J Haematol*. 2015;168(1): 14-25.

54. Bochtler T, Hegenbart U, Kunz C, et al. Translocation t(11;14) is associated with adverse outcome in patients with newly diagnosed AL amyloidosis when treated with bortezomib-based regimens. *J Clin Oncol*. 2015;33(12): 1371-1378.

55. Forloni G, Colombo L, Girola L, Tagliavini F, Salmona M. Anti-amyloidogenic activity of tetracyclines: studies in vitro. *FEBS Lett*. 2001; 487(3):404-407.

56. Giorgetti S, Raimondi S, Pagano K, et al. Effect of tetracyclines on the dynamics of formation and destructuration of beta2-microglobulin amyloid fibrils. *J Biol Chem*. 2011;286(3):2121-2131.

57. Arendt BK, Ramirez-Alvarado M, Sikkink LA, et al. Biologic and genetic characterization of the novel amyloidogenic lambda light chain-secreting human cell lines, ALMC-1 and ALMC-2. *Blood*. 2008;112(5):1931-1941.